Journal of Sound and Vibration (1999) **226**(5), 1011–1028
Article No. jsvi.1999.2376, available online at http://www.idealibrary.com on IDEAL®

STUDY OF THE DISCHARGE OF WEAK SHOCKS FROM AN OPEN END OF A DUCT

H. D. KIM

Department of Mechanical Engineering, Andong National University, Songchun-dong, Andong 760-380, *Korea*

AND

T. SETOGUCHI

Department of Mechanical Engineering, Saga University, Honjo-machi, Saga-shi, Saga 840, *Japan*

(*Received* 6 *March* 1998, *and in final form* 1 *April* 1999)

Shock discharge from a duct exit is often encountered in many engineering practices and usually gives rise to an annoying noise problem similar to a sonic boom. Such a noise can have hazardous effects on human beings, as well as structures in the vicinity, unless proper control strategies are developed. The objective of the current work is to characterize the impulse wave caused by a weak shock discharged from an open end of a duct. Experiments were performed using an open-ended shock tube for shock Mach number of 1·02–1·45. Computational analysis was applied to model the unsteady flow field by application of axisymmetric, inviscid, compressible equations. A total variation diminishing (TVD) numerical scheme was used to solve the conservation equation system. The effect of a baffle plate, installed at the duct exit, on the impulse wave was investigated both experimentally and by numerical calculation. The results of the experiments were in good agreement with the results of numerical calculations. The results showed that the baffle plate affects the strength of the impulse wave only when its diameter is less than 3 times the duct diameter. With the diameter of the baffle plate less than 3 times the duct diameter, the strength of an impulse wave for a given shock Mach number increases when the baffle plate becomes larger. The impulse wave has a directivity to the centerline of the duct. It was found that for prediction of the impulse wave aero-acoustical theory should be used only at distances larger than four times the duct diameter.

1. INTRODUCTION

Unsteady compressible fluid flow through a duct is often encountered in many engineering applications and has been investigated by many researchers. When a pressure wave generated inside a duct is discharged from an open end of the duct, an impulsive wave, that is usually characterized by high sound pressure level of short duration, forms at the vicinity of the exit of the duct. Inside the duct pressure fluctuations occur due to successive reflections of the pressure waves from the exit and entrance of the duct.

0022-460X/99/401011 + 18 $30.00/0

The discharge problem of a shock wave from an open end of a duct has been associated with a variety of unsteady internal flow devices, for instance, gun muzzles [1], diesel engine exhaust mufflers [2], dynamic pressure exchangers [3], pulse combustors [4], pulse jet filters [5], and etc. The characteristics of an impulse wave resulting from a shock discharge should be fully understood in order to estimate the performance of such unsteady flow devices.

Pennelegion *et al.* [6] and Stollery *et al.* [7] investigated the shock discharge phenomenon with a specified Mach number, and provided the spatial distributions for the strength of the resulting impulse waves. However, they did not involve the effect of the shock Mach number and duct configuration on the strength of the impulse wave.

A similar impulse wave phenomenon can be found in high-speed railway train/tunnel systems which have been under development in many countries in recent years. When a high-speed train enters a tunnel, a compression wave is formed ahead of the train and propagates toward the exit of the tunnel. A part of the compression wave is reflected back from the exit of the tunnel as an expansion wave. A complex wave interaction occurs inside the tunnel due to successive reflections of the pressure waves at the exit and entry to the tunnel. These pressure waves cause pressure transients resulting in fluctuating loads on the running train and thus discomfort to passengers as well as instability to the running train [8].

A part of the compression wave is discharged from the exit of the tunnel and gives rise to an impulse noise similar to a sonic boom. Such an impulse noise was not an important issue in the past when the speed of trains was not high. However, with the increase in the speed of trains in recent years, the impulse noise has become a new type of environmental problem. It is thus necessary that both the pressure transients and impulse noise should be minimized by an appropriate means.

In order to evaluate the pressure transients and impulse noise, the detailed reflection and discharge processes of the pressure wave at the open end of the tunnel should be clarified. In general, a pressure wave with a finite wave length does not perfectly reflect from an open end of a duct. An open-end correction may, therefore, be required to modify an otherwise perfect reflection from the exit of the duct [9], in order to evluate the impulse noise and pressure fluctuation.

Kim *et al.* [10] investigated the open-end correction of a shock wave reflection from an open end of a duct with and without a baffle plate, and showed that the open-end correction can be influenced by only a small baffle plate. They also presented new empirical equations for an open-end correction relevant to weak shock discharges from the exit of a duct.

Weak shock discharge phenomenon is of importance in many practical engineering problems. However, there are only a few reports on this topic [11]. The existing data are too sparse to improve current understanding of the shock discharge problem from the exit of a duct. Clearly, much more work is required before it can be said that the impulse noise is both understood and, hopefully, minimized.

In the current work, an experiment was performed using a simple shock tube with an open end, and numerical calculations were carried out to predict the corresponding unsteady axisymmetric inviscid comprerssible flow fields. The effects

of a baffle plate on the strength of the impulse wave were investigated over the range of the weak shock Mach number from 1·01 to 1·45. Some characteristics were established of the weak shock discharging from the open end of a duct with and without a baffle plate. It was also found that the strength of the pulse wave was strongly influenced by the baffle plate when the diameter was smaller than three times the duct diameter.

2. EXPERIMENT AND MEASUREMENT

Static pressures were measured at several stations along the shock tube wall to characterize the propagating shock waves. The simple open-ended shock tube (see Figure 1) had a diameter (D) of 66 mm and a total length of about 3·8 m (the length of the driven section: 2·2 m). Calibrated pressure transducers were mounted flush on the wall of the shock tube. A sheet of cellophane of thickness 0·03 mm was used as a diaphragm, which was manually ruptured. The initial pressure ratio of the shock tube was set to obtain shock Mach number, M, below 1·45, the driven air being initially at atmospheric pressure and room temperature. A baffle plate of diameter D_b was installed at the exit of the shock tube. In particular, static pressures at the positions of 322 mm (the measuring point ①) and 187 mm (the measuring point ②) from the exit of the shock tube were employed to establish the shock Mach number M (see Figure 1).

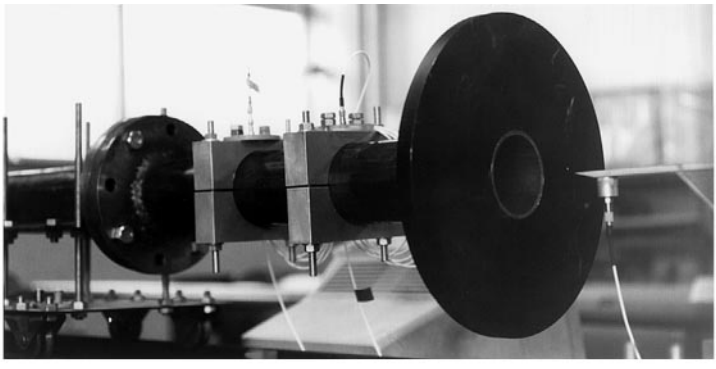

Figure 1. Picture showing the experimental apparatus and schematic.

Another pressure transducer was installed on a wedge, with a sharp leading edge to monitor the impulse wave at far field locations (r, θ) beyond the duct exit. The wedge was movable to establish the local direction of the impulse wave. Output of the pressure transducer was recorded on an X–Y recorder by way of a wave memory. The pressure transducers were statically calibrated before each test. The uncertainty in pressure measurements was estimated to be below $\pm 2\%$.

3. COMPUTATIONAL ANALYSIS

Figure 2 shows schematically the weak shock flow discharged from the duct exit. Defining the pressure rise of the propagating shock in the duct as $\Delta p^*(=p^* - p_1)$, where the pressure upstream of the propagating shock is p_1, and the pressure just downstream of the shock is p^*. In order to quantify the strength of the impulse wave, Δp_m is employed (see Figure 2), where Δp_m is defined as (p_m/p_1)-1 (p_m is a maximum pressure of the impulse wave).

Unsteady axisymmetric inviscid conservation equations are solved numerically by assuming a perfect gas ($\gamma = 1{\cdot}4$),

$$\frac{\partial U}{\partial t} + \frac{\partial F}{\partial x} + \frac{\partial G}{\partial y} + W = 0, \tag{1}$$

$$U = \begin{bmatrix} \rho \\ \rho u \\ \rho v \\ e \end{bmatrix}, \quad F = \begin{bmatrix} \rho u \\ \rho u^2 + p \\ \rho uv \\ (e + p)u \end{bmatrix}, \quad G = \begin{bmatrix} \rho u \\ \rho uv \\ \rho v^2 + p \\ (e + p)v \end{bmatrix}, \quad W = \frac{1}{y} \begin{bmatrix} \rho v \\ \rho uv \\ \rho v^2 \\ (e + p)v \end{bmatrix},$$

where x is the longitudinal distance, y the radial distance, ρ the density and, u and v the velocity components for x and y directions respectively. The total energy e per unit volume of the gas is expressed by the sum of the kinetic energy and the internal energy as follows:

$$e = \frac{p}{\gamma - 1} + \rho\left(\frac{u^2 + v^2}{2}\right). \tag{2}$$

Equation (1) is closed by the thermal equation of state of a perfect gas, $p = \rho RT$, where T is the temperature. In the computations, equation (1) is rewritten in non-dimensional form by referring the quantities, the pressure, density, etc., to atmospheric conditions and the diameter of the duct.

$$p' = \frac{p}{p_1}, \quad \rho' = \frac{\rho}{\rho_1}, \quad u' = \frac{u}{a_1\sqrt{\gamma}}, \quad v' = \frac{v}{a_1\sqrt{\gamma}}, \quad t' = \frac{t}{(D/a_1)\sqrt{\gamma}}, \quad x' = \frac{x}{D}, \quad y' = \frac{y}{D}. \tag{3}$$

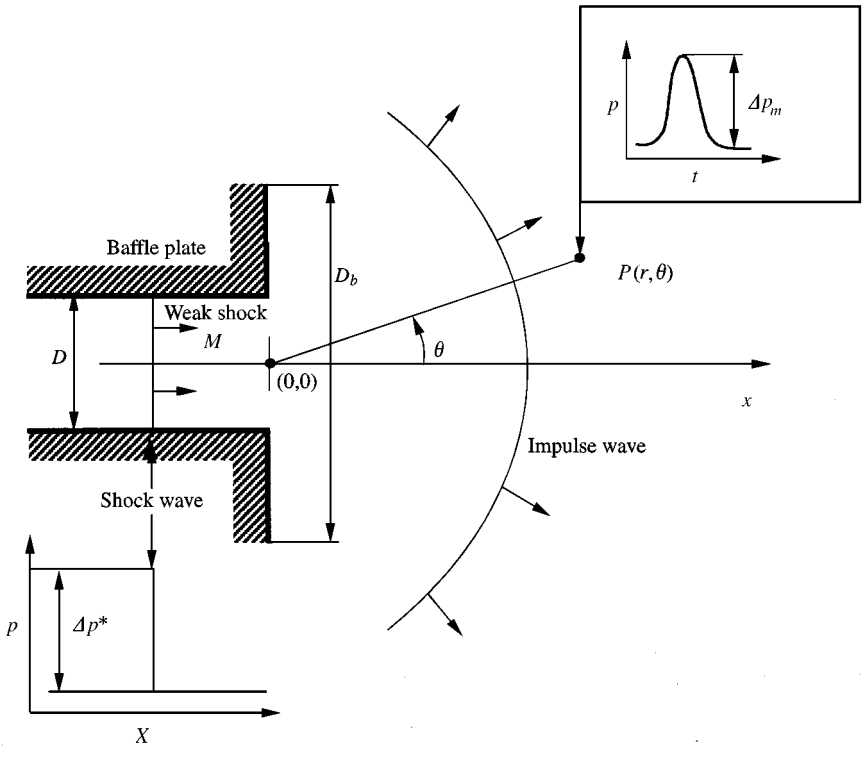

Figure 2. Flow field for computation.

The superscript (′) indicating the non-dimensional quantities was omitted for the sake of simplicity. The resulting non-dimensional form of equation (1) was solved numerically using the Harten–Yee TVD scheme [12]. The second order symmetric total variation diminishing (TVD) was incorporated into the operator splitting technique which was suggested by Sod [13]. For setting up the initial conditions, a normal shock with its overpressure p^* was assumed to be discharged from the duct exit. The inflow conditions upstream, the symmetric conditions at the centerline of the duct, the slip-wall conditions at the duct walls, and the outflow conditions downstream were used as the boundary conditions. A square grid system with a mesh size of $\Delta x = \Delta y = 2{\cdot}0$ mm was used to obtain the pressure waves discharged from the open end of the shock tube.

4. RESULTS AND DISCUSSION

4.1. EXPERIMENTAL RESULTS

According to the previous work [14], the strength of an impulse wave due to a weak shock discharge from an open end of a duct reduces to half strength at a distance from the open end in the region of $r/D > 2{\cdot}0$. The current experimental data were taken to investigate the characteristics of the impulse wave for the far field where $r/D > 2{\cdot}0$.

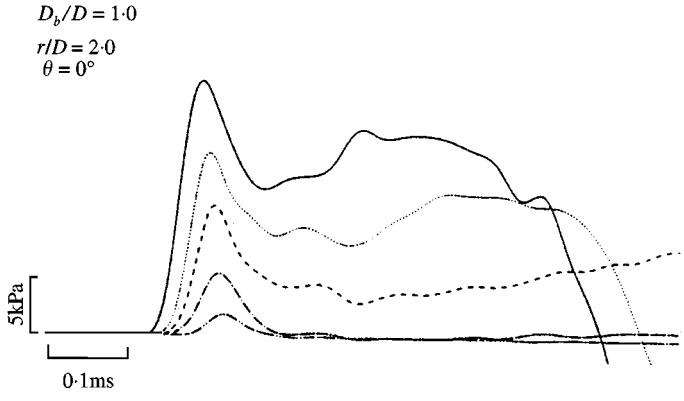

Figure 3. Pressure history of impulse wave. $D_b/D = 1{\cdot}0$, $r/D = 2{\cdot}0$ and $\theta = 0°$. —— $M = 1{\cdot}42$; ..... $M = 1{\cdot}37$; - - - - $M = 1{\cdot}26$; –·–·–·– $M = 1{\cdot}16$; –··–··–··– $M = 1{\cdot}05$.

Figure 3 shows the measured impulse wave forms for different shock Mach numbers ($D_b/D = 1{\cdot}0$, $r/D = 2{\cdot}0$, and $\theta = 0°$). The strength of the impulse wave, that is, the first peak pressure seen in the wave forms, increases with an increase in the shock Mach number M. The high pressures downstream of the first peak for higher Mach numbers are due to the shock-induced flows.

For baffle plate with different D_b/D, the effect of the shock Mach number on the strength of impulse wave is found in Figure 4(a, b). It is found from Figure 4(a) that for a given value of D_b/D, Δp_m increases with an increasing M. For a given shock Mach number, Δp_m increases with increasing D_b/D provided D_b/D is below 3·0. This results from the fact that the discharged shock energy is spatially limited to a smaller volume when the baffle plate is installed at the duct exit.

For a given shock Mach number, Δp_m does not vary with D_b/D when D_b/D is greater than 3·0. The impulse wave is influenced by the expansion waves reflected from the baffle plate. Here it should be, however, noted that the effect of D_b/D on Δp_m can vary with r/D.

The non-dimensional strength $\Delta p_m/\Delta p^*$ of the impulse wave is represented in Figure 4(b). For the same Mach number M, $\Delta p_m/\Delta p^*$ increases with an increase in D_b/D when it is below 3·0, but no longer varies for $D_b/D > 3{\cdot}0$. It is interesting to note that the $\Delta p_m/\Delta p^*$ has a minimum value for a certain Mach number M. This is not well understood at present. Further work is required to gain more insight into the details of the processes involved.

In order to show the effect of r/D on $\Delta p_m/\Delta p^*$, Figure 5 represents the relationship between M and $\Delta p_m/\Delta p^*$ along the duct centerline. For both the cases of $D_b/D = 1{\cdot}0$ (no baffle plate) and $D_b/D = 5{\cdot}5$, $\Delta p_m/\Delta p^*$ at $r/D = 2{\cdot}0$ decreases and then increases with an increasing M after having a minimum value for a certain Mach number, as described in Figure 4. However, this tendency for change does not occur in the case of $r/D = 4{\cdot}0$. The effect that the baffle plate has on the $\Delta p_m/\Delta p^*$ appears to be insignificant at the location of a large r/D far away from the duct exit. At such a large r/D, the reflected expansion wave may have time enough to catch up with the propagating impulse wave, thus cancelling out the baffle plate

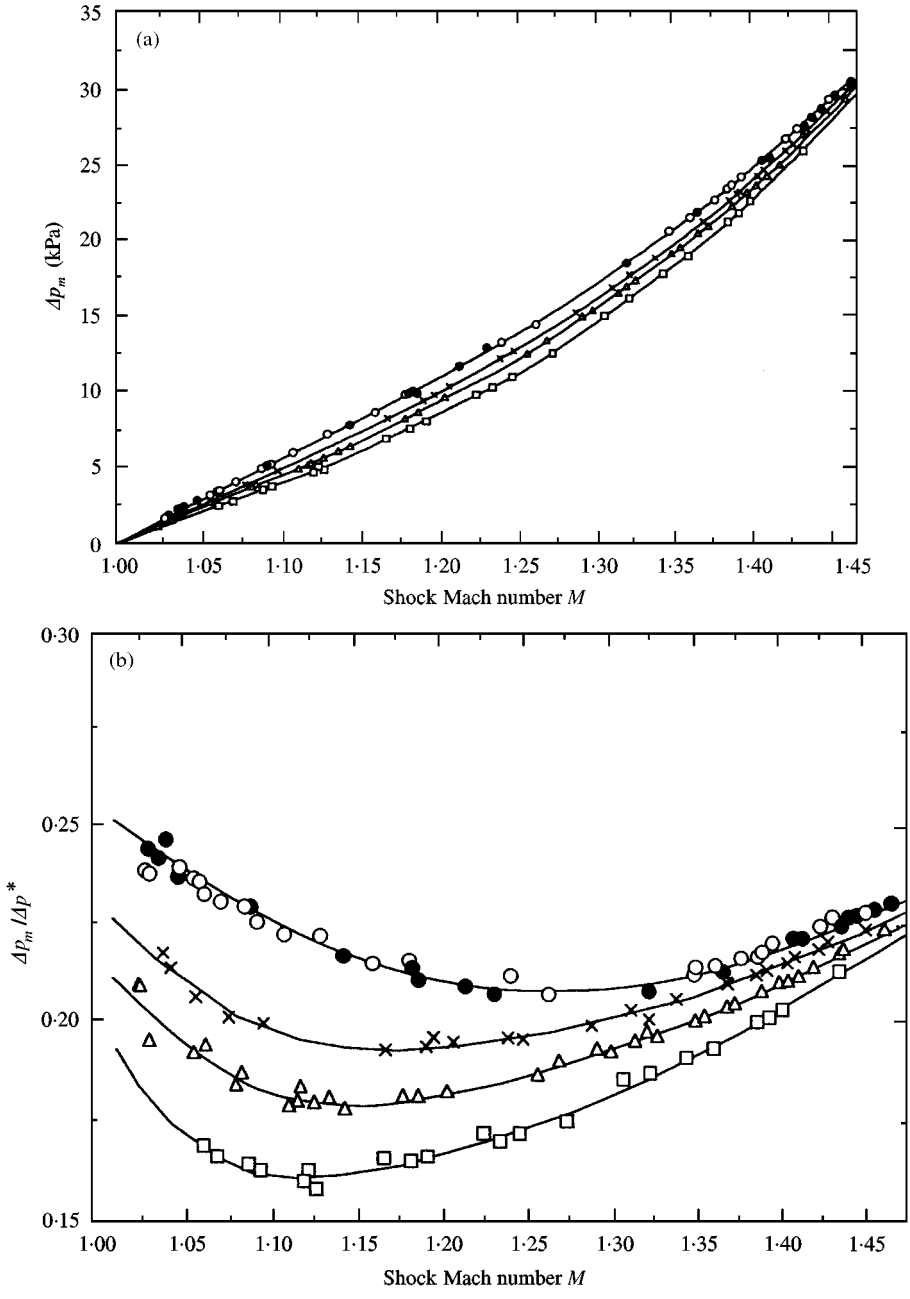

Figure 4. The relationship between the shock Mach number and the strength of impulse wave for various baffle plates; (a) The strength of impulse wave. $r/D = 2{\cdot}0$, $\theta = 0^\circ$; —□— $D_b/D = 1{\cdot}0$; —△— $D_b/D = 1{\cdot}5$; —×— $D_b/D = 2{\cdot}0$; —○— D_b/D 3·0; —●— $D_b/D = 5{\cdot}5$. (b) Non-dimensional strength of impulse wave $r/D = 2{\cdot}0$, $\theta = 0^\circ$; —□— $D_b/D = 1{\cdot}0$; —△— $D_b/D = 1{\cdot}5$; —×— $D_b/D = 2{\cdot}0$; —○— D_b/D 3·0; —●— $D_b/D = 5{\cdot}5$.

effect. Then, the $\Delta p_m/\Delta p^*$ monotonously decreases with an increasing M. The present experimental data show only negligible effects of the baffle plate for large Mach numbers.

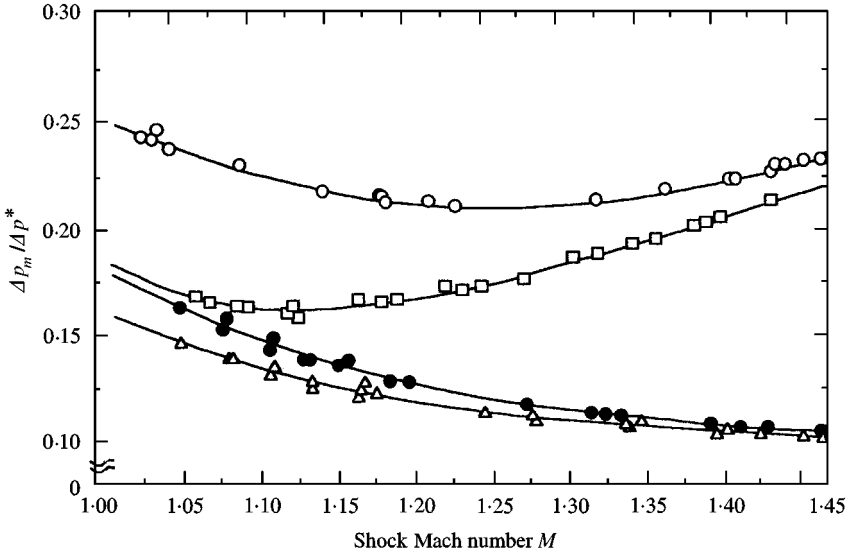

Figure 5. The relationship between $\Delta p_m/\Delta p^*$ and M showing the effect of the distance from the duct exit. $D_b/D = 1{\cdot}0$, $\theta = 0°$; —□— $r/D = 2{\cdot}0$; —△— $r/D = 4{\cdot}0$; $D_b/D = 5{\cdot}5$, $\theta = 0°$; —○— $r/D = 2{\cdot}0$; —●— $r/D = 4{\cdot}0$.

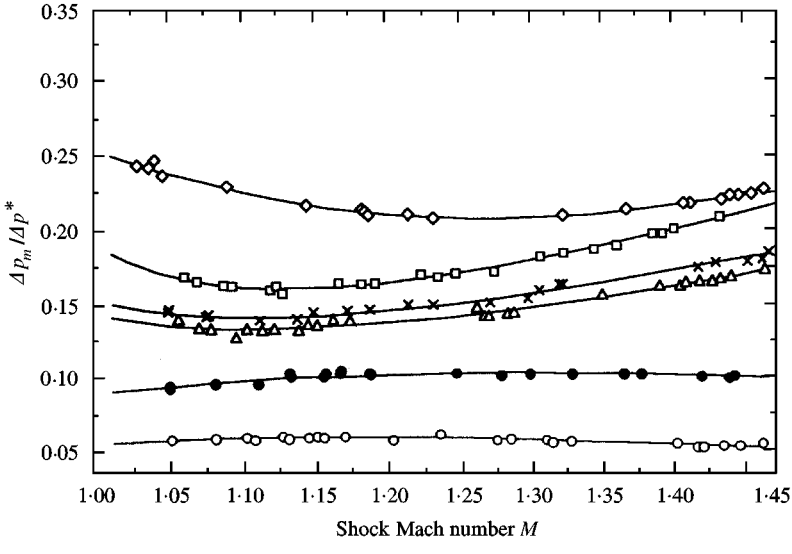

Figure 6. The relationship between $\Delta p_m/\Delta p^*$ and M for three azimuth angles. $D_b/D = 1{\cdot}0$, $r/D = 2{\cdot}0$; —□—: $\theta = 0°$; —△—: $\theta = 45°$; —○—: $\theta = 90°$. $D_b/D = 5{\cdot}5$, $r/D = 2{\cdot}0$; —◇—: $\theta = 0°$; —×—: $\theta = 45°$; —●—: $\theta = 90°$.

The directional sensitivity of the impulse wave is shown in Figure 6. For the case of $\theta = 90°$, $\Delta p_m/\Delta p^*$ appears nearly constant over all tested Mach numbers. Some directional sensitivity of the impulse wave appears near the duct centerline. For $\theta = 45°$, the baffle plate seems to affect negligibly the directional sensitivity of the impulse wave.

4.2. NUMERICAL RESULTS

For an infinite baffle plate, Figure 7 shows the pressure variations along the duct axis for six non-dimensional time (t') intervals of 0·291, where t' is defined as $ta_1/(D\sqrt{\gamma})$, as indicated in equation (3). The $x/D = 0$ variable originates at the exit of the duct. A clear peak in the impulse wave is not found at the non-dimensional time $t' = 0{\cdot}582$, the shock just being discharged from the open end of the duct. For $t' = 0{\cdot}873$, the peak pressure appears at $x/D = 0{\cdot}7$, and then propagates toward the surrounding with appreciable attenuation. At the same time, an expansion wave propagates back inside the duct, and for $t' = 1{\cdot}455$, the head of the expansion wave is located at $x/D = -1$.

Figure 8 shows the iso-pressure contours of the shock discharge flow field for a certain non-dimensional time t'. The impulse wave forms are all similar to a semi-spherical shape, and the peak pressure in these impulse waves seems to occur on the duct centerline. For M to decrease, the impulse wave form appears to be closer to a semi-spherical shape, leading to a sound wave propagation from a source. The reflected expansion wave propagates back toward the duct entrance as a plane wave. It is also found that the lowest pressure on the duct centerline occurs just at the exit plane of the duct, consequently showing a vortex ring there.

A comparison of measured and computed impulse waves at $x/D = 2{\cdot}0$ is shown in Figure 9, where the shock Mach number M is 1·25. The peak pressure Δp_m of the impulse waves for the two results is the same and is about 13 kPa, although the

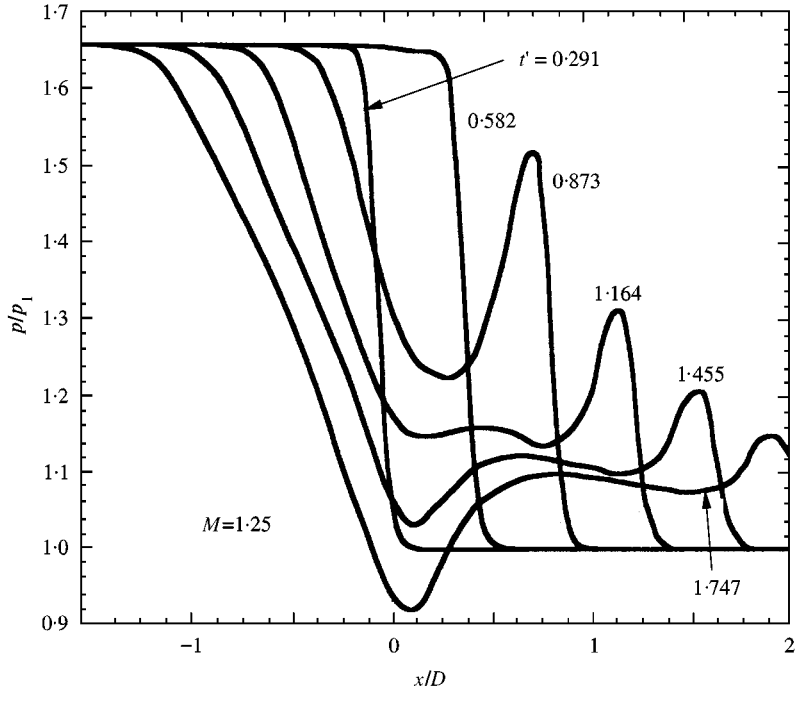

Figure 7. Pressure distribution along the duct axis.

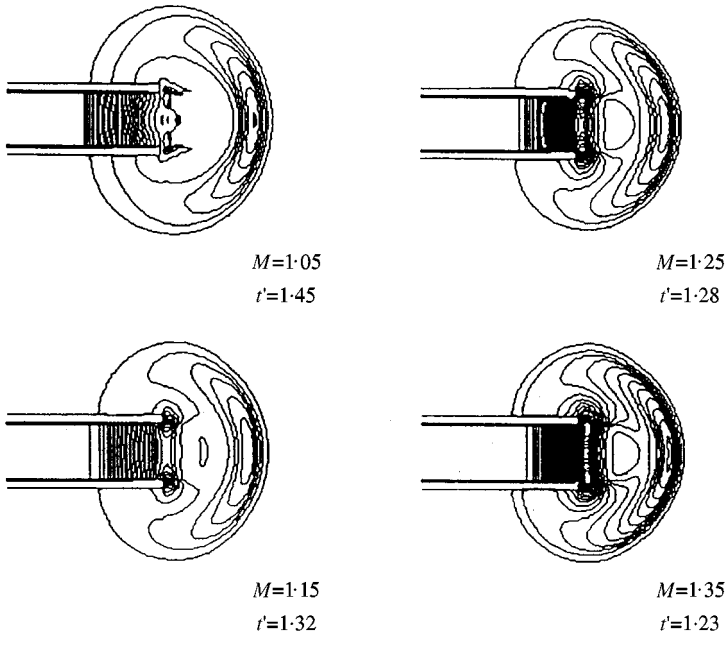

Figure 8. Iso-pressure contours at a non-dimensional time; (a) $M = 1{\cdot}05$, (b) $M = 1{\cdot}15$, (c) $M = 1{\cdot}25$, and (d) $M = 1{\cdot}35$; $D_b/D = 1{\cdot}0$ for all cases.

detailed wave forms are somewhat different from each other. Good agreement was obtained for the peak pressures.

Figure 10 shows the effects of the baffle plate and shock Mach number on the peak pressure p_m/p_1 of the impulse wave along the duct centerline at $x/D = 2{\cdot}0$. It was found that the peak pressure depended on the size of baffle plate as well as the shock Mach number. For a given Mach number the peak pressure increases as the baffle plate becomes larger, but the peak pressure seems to no longer increase as the baffle plate goes beyond a certain size [10]. Experimental results also showed that the peak pressure no longer varies when $D_b/D > 3{\cdot}0$.

Figure 11 shows the relationship between the numerically derived non-dimensional peak pressure $\Delta p_m/\Delta p^*$ and shock Mach number M. It was found that $\Delta p_m/\Delta p^*$ depends on the shock Mach number and shock overpressure Δp^*. It should be noted that for all the cases with the baffle plate, the $\Delta p_m/\Delta p^*$ has a minimum value at a certain Mach number, leading to good agreement with the present experimental results. With no baffle plate, the minimum value of 0·169 occurs at $M = 1{\cdot}15$. This means that with no baffle plate, the non-dimensional peak pressure of an impulse wave can be minimized only by properly adjusting the shock Mach number.

The numerically derived peak pressure of the impulse wave along the duct centerline attenuates with the propagating distance (see Figures 12 and 13). As the distance from the duct exit increases, the effect of the baffle plate on the peak pressure becomes insignificant. For example, for $M = 1{\cdot}45$ and no baffle plate, the peak pressure at $x/D = 4{\cdot}0$ is only about 40% of that at $x/D = 2{\cdot}0$.

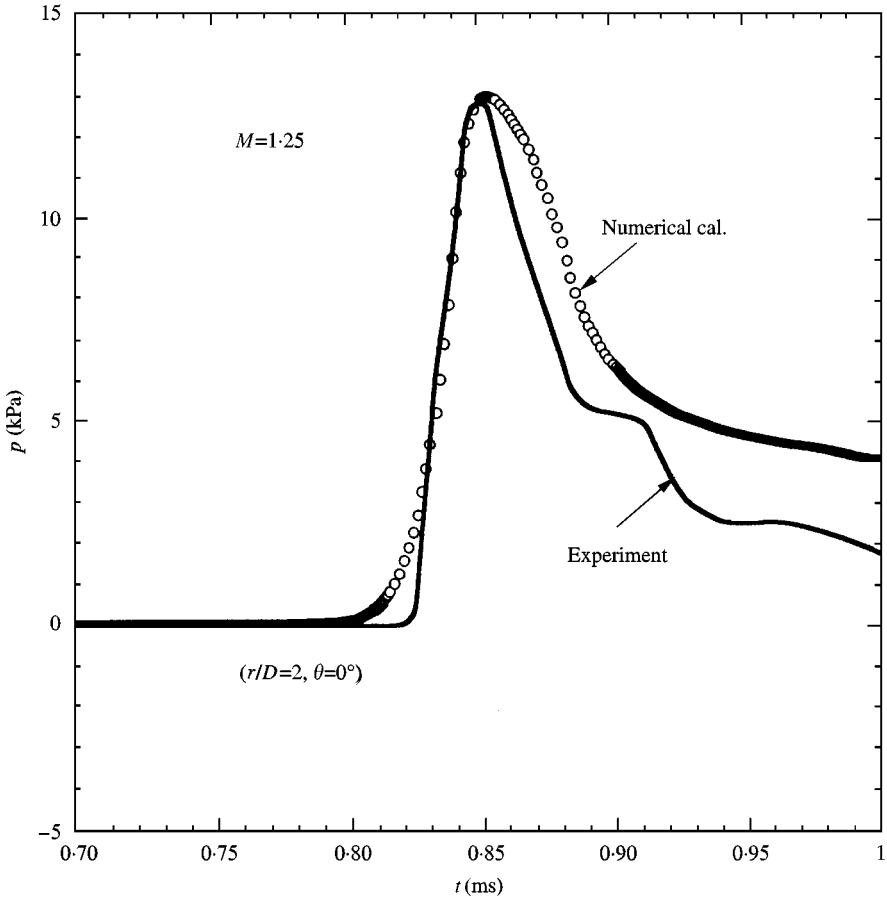

Figure 9. Measured and computed pressure histories. $M = 1{\cdot}25$, $r/D = 2{\cdot}0$ and $\theta = 0°$.

According to aero-acoustical theory [14], the strength of an impulse wave with an infinite baffle plate can be expressed by

$$\frac{\Delta p_m}{\Delta p^*} = \frac{D^2}{8\gamma\,\Delta l}, \tag{4}$$

where Δl is the open-end correction length for the emission of a sound wave from a duct exit. The Δl for a discharging shock wave was not yet fully understood. Moreover, the above equation (4) does not include the directional influence on the impulse wave.

Figure 14 shows a comparison of the results computed by the current numerical method and predicted by the above equation (4), where $\Delta l = 0{\cdot}4250$ [15]. It was found that the aero-acoustical theory failed in predicting the strength of the impulse wave near the exit of the duct. This is mainly due to the directional sensitivity of the impulse wave. However, the two sets of results agree well at a location far away from the duct exit. The current results imply that for prediction of an impulse noise, the aero-acoustical theory should be applied only in the region of $x/D > 4{\cdot}0$.

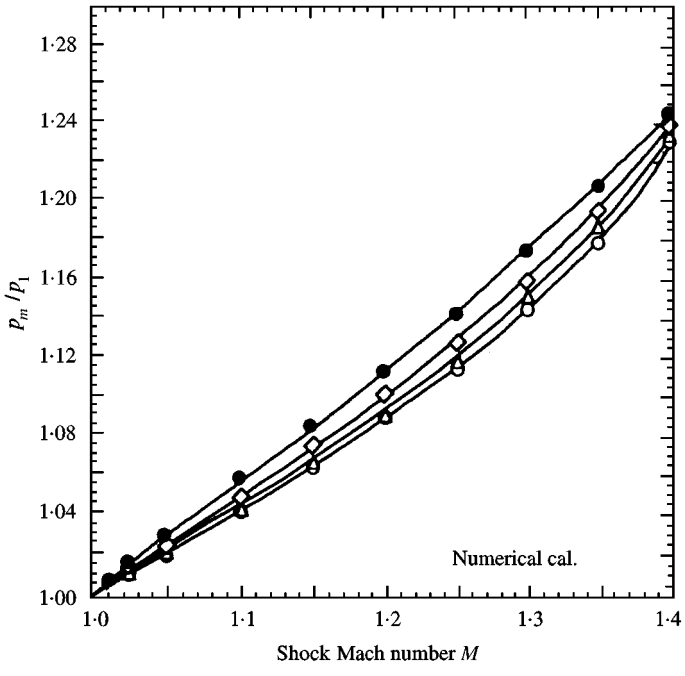

Figure 10. p_m/p_1 versus M at $x/D = 2{\cdot}0$. ○: $D_b/D = 1$; △: 1·5; ◇: 2·0; ●: infinite.

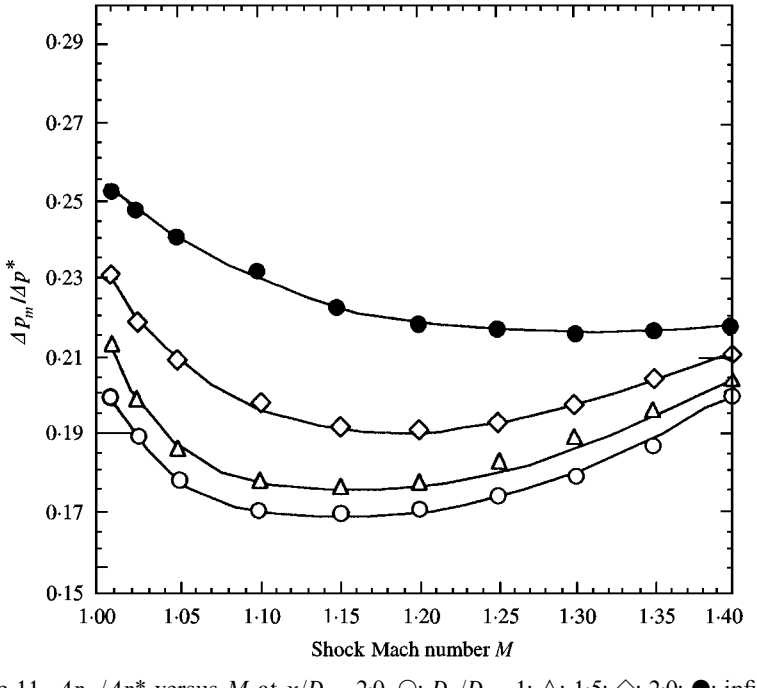

Figure 11. $\Delta p_m/\Delta p^*$ versus M at $x/D = 2{\cdot}0$. ○: $D_b/D = 1$; △: 1·5; ◇: 2·0; ●: infinite.

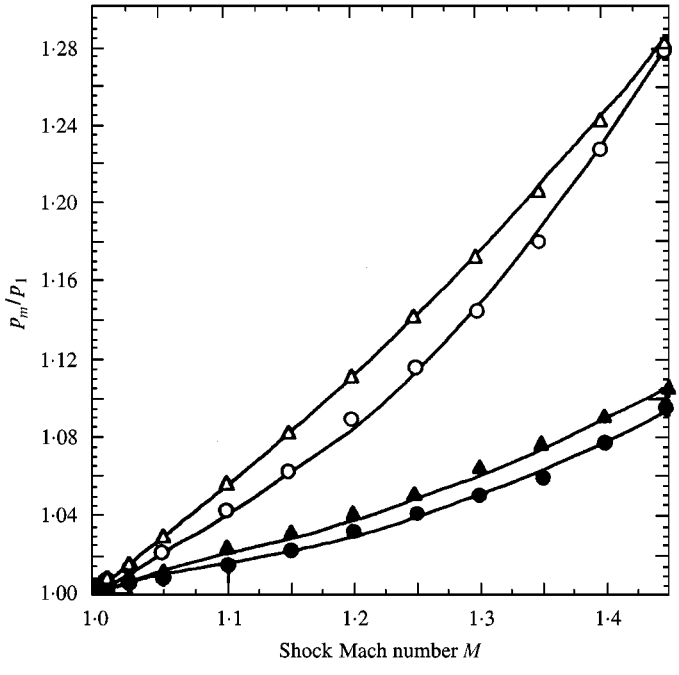

Figure 12. Dependence of the distance from the duct exit on p_m/p_1. ○: $D_b/D = 1(x/D = 2)$; △: Infinite $(x/D = 2)$; ●: $D_b/D = 1(x/D = 4)$; ▲: Infinite $(x/D = 4)$.

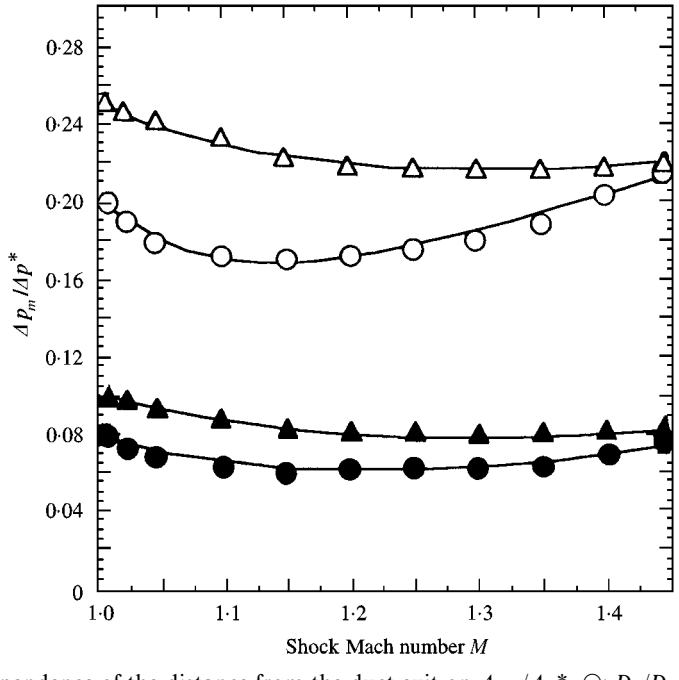

Figure 13. Dependence of the distance from the duct exit on $\Delta p_m/\Delta p^*$. ○: $D_b/D = 1$ $(x/D = 2)$; △: Infinite $(x/D = 2)$; ●: $D_b/D = 1$ $(x/D = 4)$; ▲: Infinite $(x/D = 4)$.

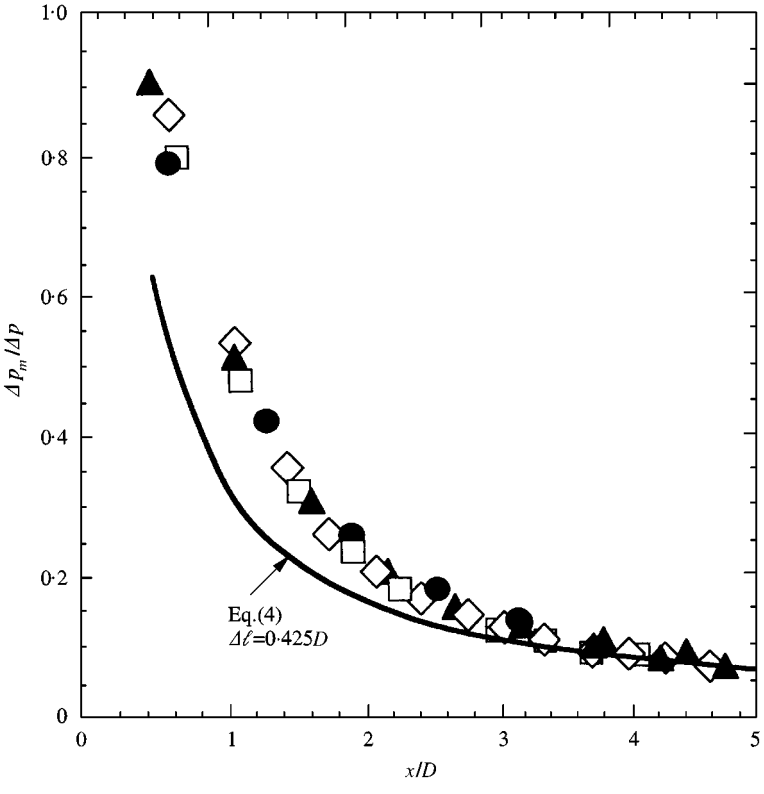

Figure 14. Variation of the impulse wave strength with the distance from the duct exit. Infinite baffle plate. ●: $M = 1{\cdot}01$; ▲: $M = 1{\cdot}1$; □: $M = 1{\cdot}25$; ◇: $M = 1{\cdot}4$; —: Aero-acoustic theory.

For both the cases with and without an infinite baffle plate, Figure 15 shows the directional sensitivity of an impulse wave at a constant distance of $r/D = 2{\cdot}0$. For all the three azimuth angles investigated, the impulse wave appears stronger for the case with the infinite baffle plate than that without the baffle plate. It is found that the $\Delta p_m/\Delta p^*$ at $\theta = 45^\circ$ becomes stronger with an increasing M, while at $\theta = 90^\circ$ it is nearly constant regardless of the shock Mach number.

As a consequence of the foregoing results, new empirical equations are presented describing the strength of the impulse wave at a certain location $(r/D, \theta)$ of far field from the duct exit. The $\Delta p_m/\Delta p^*$ can be expressed by equations (5) and (6) for the cases with and without an infinite baffle plates respectively,

$$\frac{\Delta p_m(r, \theta)}{\Delta p^*} = \frac{1}{8K_1(r/D)}, \tag{5}$$

$$\frac{\Delta p_m(r, \theta)}{\Delta p^*} = \frac{1}{16K_2(r/D)}, \tag{6}$$

where K_1 and K_2 are the coefficients which can be related to the local flow direction and open-end correction of an impulse wave. Equations (5) and (6) are based upon

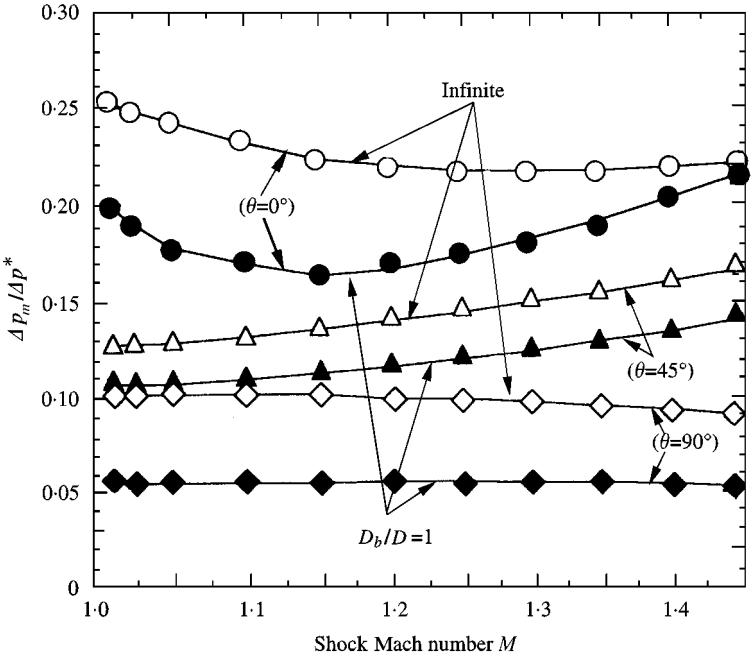

Figure 15. Effect of θ on $\Delta p_m/\Delta p^*$.

the aero-acoustical theory. Using the results of the current computations, the above coefficients K_1 and K_2 are plotted against shock Mach number (see Figure 16). With known values of M and θ, the strength of an impulse wave can be found from the modified aero-acoustic equations (5) and (6).

5. CONCLUSIONS

The present paper describes the characteristics of an impulse wave caused by a weak shock discharged from an open end of a duct. Experiments were performed using an open-ended shock tube over the shock Mach number range from 1·02 to 1·45. Computational analysis was applied to model the flow field subject to unsteady, axisymmetric, inviscid, compressible equations. A TVD numerical scheme was used to solve the conservation equation system. The effect of a baffle plate, installed at the duct exit, on the impulse wave was investigated both experimentally and numerically. The results of the experiments were in good agreement with the results of the numerical calculations. The results showed that the baffle plate affects the strength of the impulse wave only when its diameter is less than 3 times the duct diameter. With the diameter of the baffle plate less than 3 times the duct diameter, the strength of an impulse wave for a given shock Mach number increases as the baffle plate became larger. It is found that the peak pressure of an impulse wave has a minimum value for a certain shock Mach number when it is non-dimensionalized by the shock overpressure. The impulse wave has a directivity to the centerline of the duct. It is found that for prediction of

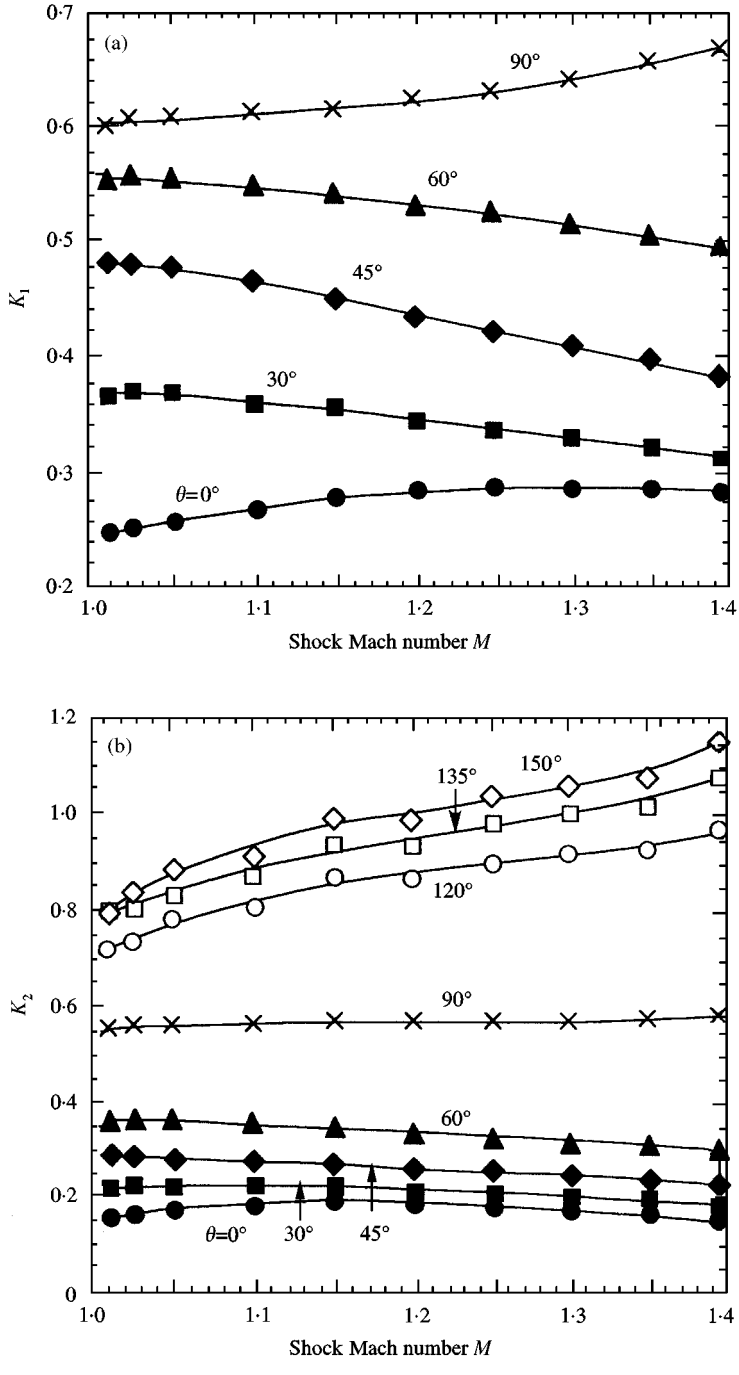

Figure 16. Coefficients K_1 and K_2 versus M; (a) infinite baffle plate, and (b) no baffle plate.

the strength of an impulse wave, aero-acoustical theory should be employed only for displacements downstream of the duct exit greater than four times the duct diameter.

REFERENCES

1. G. Klingenberg and J. M. Heimerl 1992 *Progress in Astronautics and Aeronautics*, AIAA Educational Series. Gun muzzle blast and flash.
2. N. Sekine, N. S. Matsumura, K. Aoki and K. Takayama 1989 in 17*th International Symposium on Shock Wave and Shock Tubes*, 671–676. New York: American Institute of Physics. Generation and propagation of shock waves in the exhaust pipe of a four cycle automobile engine.
3. J. A. C. Kentfield 1993 *Nonsteady*, *One-Dimensional*, *Internal*, *Compressible Flows* (*Theory and Applications*), *Chapter* 7. *Oxford University Press.*
4. *B. T. Zinn* 1985 *Mechanical Engineering. American Society of Mechanical Engineers* **107**(8), 36–41. Pulsating combustion.
5. J. A. C. Kentfield and L. C. V. Fernandes 1990 American Society of Mechanical Engineers Paper No. 90-GT-84. Further development of an improve pulse, pressure gain, gas-turbine combustor.
6. L. Pennelegion and J. F. Grimshaw 1979 in 12*th International Symposium on Shock Tubes and Waves*, 349–358. Jerusalrem: The Magnes Press. The diffraction of the blast wave emerging from a conical nozzle driven by compressible gas.
7. J. L. Stollery, K. C. Phan and K. P. Garry 1981 in 13*th International Symposium on Shock Tubes and Waves*, 781–789. State University of New York, Albany. Simulation of blast fields by hydraulic analogy.
8. S. Raghunathan, H. D. Kim and T. Setoguchi 1998 *Progress in Aerospace Science* **34**(1), 1–44. Pergamon Press. Impulse noise and its control.
9. G. Rudinger 1995 Journal of Applied Physics **26**(11), 1339–1341. Improved wave diagram procedure for shock reflection from an open end of a duct.
10. H. D. Kim and T. Setoguchi 1998 *American Institute of Aeronautics and Astronautics Journal*. Weak shock reflection from an open end of a tube with baffle plate (to be published).
11. G. Rudinger 1957 *Journal of Fluid Mechanics* **3**(1), 48–66. The reflection of pressure wave of finite amplitude from an open end of a duct.
12. H. C. Yee 1987 *NASA TM*-89464. Upwind and symmetric shock capturing schemes.
13. G. A. Sod 1977 *Journal of Fluid Mechanics* **83**, 785–794. A numerical study of a converging cylindrical shock.
14. W. K. Blake 1986 *Mechanics of Flow -Induced Sound and Vibration* 1. New York: Academic Press.
15. Y. Nomura 1960 *Journal of Physical Society of Japan* **15**(7), 510–517 On the acoustic radiation from a flanged circular pipe (in Japanese).

APPENDIX I: NOMENCLATURE

a	speed of sound
D	diameter
e	total energy per unit volume
M	shock wave Mach number
Δl	open-end correction length
p	static pressure
r	distance
t	time
u	velocity component in x-direction
v	velocity component in y-direction
x	longitudinal distance in cylindrical coordinate
y	radial distance in cylindrical coordinate
γ	ratio of specific heats

ρ density
θ azimuth angle (deg.)

Super/Subscripts
1 *atmospheric state*
b baffle plate
m peak or maximum value
* normal shock wave overpressure
′ non-dimensional quantity